European Journal of Soil Science

European Journal of Soil Science, November 2018, **69**, 1018–1029 doi: 10.1111/ejss.12710

From microhabitat to ecosystem: identifying the biophysical factors controlling soil CO_2 dynamics in a karst shrubland

C. J. R. Lopez[a], E. P. Sánchez-Cañete[b,c], P. Serrano-Ortiz[b,d], A. López-Ballesteros[a,d], F. Domingo[a], A. S. Kowalski[b,c] & C. Oyonarte[e]

[a]*Department of Desertification and Geo-Ecology, Experimental Station of Arid Zones (EEZA-CSIC), Ctra. Sacramento s/n, 04120 La Cañada, Almería, Spain,* [b]*Inter-University Institute for Earth System Research (IISTA-CEAMA), Av. del Mediterráneo s/n, 18006, Granada, Spain,* [c]*Department of Applied Physics, University of Granada (UGR), Av. de Fuente Nueva s/n, 18071, Granada, Spain,* [d]*Department of Ecology, University of Granada (UGR), Av. de Fuente Nueva s/n, 18071, Granada, Spain, and* [e]*Department of Agronomy, University of Almería (UAL), Ctra. Sacramento s/n, 04120 La Cañada, Almería, Spain*

Summary

The soil CO_2 efflux (F_s) remains the least constrained component of the terrestrial carbon cycle; its estimates are still largely uncertain, mainly because of its considerable variation related to the many factors that interact over different temporal and spatial scales. Therefore, our aims were to: (i) identify the biophysical factors that control the soil CO_2 molar fraction (χ_s) and characterize their time-frequency patterns in a karst shrubland, (ii) explore χ_s variation with soil cover type (microhabitat) and (iii) estimate F_s at the ecosystem scale. Continuous measurements of aboveground variables, including net CO_2 exchanges at the ecosystem level, were compared with pedoclimatic variables collected from four microhabitats (*Festuca scariosa* (Lag.) Asch. & Graebn., *Hormathophylla spinosa* (L.) P. Küpfer, *Genista pumila* (Hervier) Vierh. and bare soil). The microhabitat-scale controlling factors of χ_s were identified by a top-down statistical analysis, and time-frequency patterns were analysed by wavelet spectral decomposition. Finally, F_s was upscaled from the microhabitat to the ecosystem scale by considering the spatial heterogeneity of ground cover. We determined that in addition to soil water content and temperature, which are traditionally used to predict χ_s or F_s, the wind (friction velocity) can also have a significant effect. Furthermore, the sensitivity of χ_s to the main factors identified here varied with microhabitat and season. Over a year, F_s upscaled to the ecosystem level and its uncertainty was 175 ± 13 g C m^{-2} compared with 155 ± 8 g C m^{-2} estimated from ecosystem respiration. These results provide new insight into mechanisms of soil CO_2 production and transport that question and can improve models traditionally used to quantify ecosystem CO_2 emissions.

Highlights

- Explored the variation of soil CO_2 in relation to its biophysical controlling factors.
- Used a top-down statistical analysis and a wavelet time-frequency decomposition.
- Identified controlling factors of soil CO_2 dynamics: soil water content, temperature, wind, microhabitat and season.
- Provides new insight into soil CO_2 production and transport, and improves CO_2 emission modelling.

Résumé

L'efflux de dioxyde de carbone du sol (F_s) reste la composante la moins bien cernée du cycle du carbone; ses estimations sont toujours très incertaines, principalement en raison de sa considérable variation liée aux nombreux facteurs qui interagissent sur différentes échelles temporelles et spatiales. De ce fait, nos objectifs ont été: (i) identifier les facteurs biophysiques contrôlant la fraction molaire de CO_2 du sol (χ_s) et caractériser leurs patrons temps-fréquence dans un matorral de karst, (ii) explorer la variation de χ_s selon le type de couverture du sol (microhabitat) et (iii) estimer F_s à l'échelle de l'écosystème. Des mesures continues de

Correspondence: C. J. R. Lopez. E-mail: lopezcle@gmail.com
Received 18 October 2017; revised version accepted 4 March 2018

variables aériennes, incluant les échanges de CO_2 à l'échelle de l'écosystème, ont été comparées avec des variables pédoclimatiques collectées au sein de quatre microhabitats (*Festuca scariosa* (Lag.) Asch. & Graebn., *Hormathophylla spinosa* (L.) P. Küpfer, *Genista pumila* (Hervier) Vierh. et sol nu). Les facteurs contrôlant χ_s à l'échelle du microhabitat ont été identifiés via une analyse statistique descendante et les patrons temps-fréquence ont été analysés grâce à une décomposition spectrale de wavelet. Finalement, F_s a été extrapolé de l'échelle du microhabitat à l'écosystème en considérant l'hétérogénéité spatiale de la couverture du sol. Nous avons déterminé qu'en plus du contenu en eau du sol et de la température qui sont traditionnellement utilisés pour prédire χ_s ou F_s, le vent (vitesse de friction) peut aussi avoir un effet significatif. De plus, la sensibilité de χ_s aux principaux facteurs identifiés ici a varié avec le microhabitat et la saison. Sur un an, F_s extrapolé à l'échelle de l'écosystème avec son incertitude était de 175 ± 13 g C m^{-2} comparé à 155 ± 8 g C m^{-2} estimés par la respiration de l'écosystème. Ces résultats apportent une nouvelle perspective sur les mécanismes de production et de transport du CO_2 dans le sol, remettant en question et pouvant améliorer les modèles traditionnellement employés pour quantifier les émissions de CO_2 des écosystèmes.

Introduction

Soil CO_2 efflux (F_s) remains the least constrained component of the terrestrial carbon cycle (Bond-Lamberty & Thomson, 2010) and its estimates are still largely uncertain (Bahn *et al.*, 2010). Even if a future global trend of positive feedback between F_s and climate change is likely (Hashimoto *et al.*, 2015), no consensus has been achieved yet. These uncertainties are partly attributable to the considerable variation in F_s related to the many controlling factors that interact over different temporal and spatial scales (Vargas *et al.*, 2011).

Production and transport of CO_2 control F_s. Soil CO_2 can be produced by: (i) biological respiration of roots and microorganisms (Raich & Schlesinger, 1992), (ii) photodegradation (Rutledge *et al.*, 2010), (iii) carbonate precipitation (Hamerlynck *et al.*, 2013) and (iv) geologic degassing (Etiope, 1999). Its transport is governed by: (i) molecular diffusion, determined by Fick's first law (Kowalski & Argüeso, 2011), (ii) advection, driven by wind (i.e. ventilation) (Sánchez-Cañete *et al.*, 2011) or atmospheric pressure changes (Sánchez-Cañete *et al.*, 2013), (iii) convection caused by differences in soil air buoyancy (Weisbrod *et al.*, 2009) and (iv) dissolution, according to Henry's law, and subsequent water flow (Ma *et al.*, 2014). Nevertheless, the main production and transport processes are due to biological respiration and diffusion, respectively (Šimůnek & Suarez, 1993).

Because respiration and diffusion are mainly controlled by soil temperature (T_s) and soil water content (θ), these variables have been commonly used to model F_s, either mechanistically (e.g. Pumpanen *et al.*, 2003) or statistically (e.g. Niinistö *et al.*, 2011); however, most studies continue to apply an exponential function of T_s to predict F_s (Lloyd & Taylor, 1994). In addition, other variables such as wind could have a non-negligible effect on soil–atmosphere CO_2 exchanges and carbon balance (Kowalski *et al.*, 2008) and should be incorporated into predictive models. In particular, the application of simple statistical models has been recommended to validate mechanistic models (Reichstein *et al.*, 2003).

In this research our objectives were to: (i) identify the biophysical controlling factors of the soil CO_2 molar fraction (χ_s) and characterize their time-frequency patterns in a karst shrubland, (ii) test the variation in χ_s with soil cover type (microhabitat) and (iii) estimate F_s at the ecosystem scale. We assumed that: (i) limiting factors of χ_s (T_s or θ) could change between seasons and that ventilation should be included in the modelling of χ_s based on observations at this site (e.g. Sánchez-Cañete *et al.*, 2016), (ii) variation in microclimate (T_s, θ, wind) with microhabitat could affect χ_s dynamics locally and (iii) accurate estimates of F_s at the ecosystem scale could be obtained by upscaling microhabitat measurements.

Materials and methods

Study site

This study was conducted in El Llano de los Juanes, a shrubland karstic plateau at 1600 m a.s.l. in the Sierra de Gádor (Almería, southeast Spain; 36°55′41.7″N; 2°45′1.7″W). The site is characterized by a sub-humid montane Mediterranean climate with a mean annual temperature of 12°C and mean annual precipitation of ca. 475 mm. The vegetation is diverse but sparse, with a predominance (% ground cover) of perennial shrubs (20–60 cm high): *Festuca scariosa* (Lag.) Asch. & Graebn. (18.8%), which becomes partly senescent in summer, *Hormathophylla spinosa* (L.) P. Küpfer (6.8%) and *Genista pumila* (Hervier) Vierh. (5.5%). The soil is an association of Lithic Haploxeroll and Lithic Argixeroll (Soil Survey Staff, 1999). In the topsoil (0–15 cm), the texture is silty clay, pH is slightly alkaline (7.5 ± 0.1), apparent density is 1.05 ± 0.05 g cm^{-3}, organic carbon content is 48 ± 10 g kg^{-1}, the C/N ratio is 15.1 ± 2 and calcium carbonate equivalent content is 2.1 ± 1.8%.

Environmental measurements

Continuous soil and above-surface variables were measured from January 2014 to February 2015. Soil variables were measured at 5-cm depth using a stratified random sampling; that is, by randomly

selecting sampling locations within each dominant microhabitat (*Festuca* sp., *Hormathophylla* sp., *Genista* sp. and bare soil): the soil CO_2 molar fraction (χ_s) was measured by a GMM-222 CO_2 Transmitter Module (Vaisala, Vantaa, Finland), soil water content (θ) by a CS616 water content reflectometer (Campbell Scientific, Logan, UT, USA; hereafter CSI) and soil temperature (T_s) by a thermistor (107, CSI). Measurements of T_s and χ_s were replicated spatially in the *Festuca* sp. and *Hormathophylla* sp. sites (three locations per microhabitat), but not for bare soil and *Genista* sp. This was because *Genista* sp. had a minor distribution in this ecosystem and bare soil was assumed to be the microhabitat where χ_s would be the least heterogeneous because of the absence of root respiration. At 2 cm above ground, air temperature (T_a, same sensor as T_s) and air CO_2 molar fraction (χ_a, same sensor as χ_s) were monitored in a *Festuca* sp. plant and over bare soil. Variables were measured every 30 s and stored as 30-minute averages by a data-logger (CR1000, CSI). Ecosystem-scale data were monitored by an eddy covariance tower; equipment and data quality control steps are described by Serrano-Ortiz *et al.* (2009). The variables used were: the net ecosystem exchange (NEE), relative humidity (RH), latent heat flux (F_{le}), sensible heat flux (F_h), atmospheric pressure (P_a), incident photosynthetic photon flux density (PPFD), precipitation (RAIN), wind speed (WS), friction velocity (u_*), wind direction (WD), tower-top T_a and vapour pressure deficit (VPD). Measurements were made at 10 Hz for the eddy covariance system and at 1 Hz for the rest of the variables and stored as 30-minute averages by a data-logger (CR3000, CSI). Enhanced vegetation index (EVI) values obtained at 16-day intervals at a 250-m resolution by the Terra MODIS satellite were also added to the dataset. To this end, the MOD13Q1 Image of our experimental site was downloaded from the FLUXNET server (https://fluxnet.ornl.gov/).

Preliminary data processing

The χ_s and χ_a were corrected for pressure and temperature and soil CO_2 effluxes calculated as:

$$F_s = -\rho_a k_s \frac{d\chi_c}{dz}, \quad (1)$$

where F_s is the soil CO_2 efflux (μmol m^{-2} s^{-1}), k_s is the empirical soil CO_2 transfer coefficient (m^2 s^{-1}) calibrated for this site with soil chamber measurements and equal to the soil CO_2 diffusion coefficient in the absence of production or consumption processes and non-diffusive transport in the monitored layer (Sánchez-Cañete *et al.*, 2016), ρ_a is the air molar density (μmol m^{-3}), $d\chi_c$ is the increment in CO_2 molar fraction (μmol mol^{-1}) between the atmosphere (average of bare soil and *Festuca* sp. at ca. 0 cm, 2 cm above ground in our case) and soil, and dz is the vertical gradient between the atmosphere and soil (m, 0.05 m in our case).

The online eddy covariance gap-filling and flux-partitioning tool of the Max Planck Institute for Biogeochemistry (Jena, Germany) was used to fill in missing data for NEE, F_h and F_{le} and to estimate the ecosystem respiration (R_{eco}) as a function of the tower-top T_a with the associated error (http://www.bgc-jena.mpg.de/~MDIwork/eddyproc/). The variance of measured NEE was calculated by introducing artificial gaps and repeating the gap-filling procedure, then errors in NEE balances were calculated as twice the standard deviation of the sum of variances. Gaps in the data of the remaining variables were filled by a non-parametric method based on a random forest (Stekhoven & Bühlmann, 2012).

The dataset was split into three seasons (factor SEASON): growing season of plants (negative NEE values in spring), dry season (θ below 0.15 and increasing NEE) and inter-season (rest of the year). Additional factor variables were also created to represent the soil cover type (MICROHABITAT) and sampling location (LOCATION).

Statistical modelling and ecosystem upscaling

Statistical modelling was used to identify the biophysical controlling factors of χ_s. All analyses were performed with R software v. 3.4.3 (R Core Team, 2017) and the significance level was set to 5%. Because the large number of variables was likely to introduce multicollinearity into the models (which is known to produce unstable model parametrization and hence, uninterpretable coefficients), a principal component analysis (PCA) was used to reduce the number of variables prior to modelling (detailed protocol and results in Supporting Information). Variables selected were those contributing strongly to the three first components (Figure S1, Supporting Information), which explained more than two-thirds of the variance in the data (Table S1, Supporting Information). Figure S2(a) shows the selected variables plotted in the correlation circle of the first two PCs and Figure S2(b) shows the PC scores (organized by seasons) plotted in the plane of PCs 1 and 2. Selected potential predictors of χ_s were averaged daily and standardized (centred and scaled to zero mean and unit variance); the inner transformation saved computational time, whereas the latter ensured reduced multicollinearity arising from interaction and quadratic terms, and that comparable regression coefficients could be obtained (because variables had different units). During comparison of models, the best model was always retained, as that which minimized the Akaike information criterion (AIC) or improved residual structure. We made sure that model assumptions were met during the selection process: (i) *normality*, tests for normality become sensitive to even small departures from the initial assumption when the number of observations is large, therefore inspection of the distribution of residuals was preferred; (ii) *homoscedasticity*, by extension, homoscedasticity tests generally require normality, therefore we preferred to visualize the spread of residuals against fitted values to assess this and (iii) *independence in time*. Because data were autocorrelated, the temporal dependence was modelled with a first-order autoregressive (AR1) correlation structure.

The top-down protocol of Zuur *et al.* (2009) was used to model χ_s. First, we used restricted maximum likelihood (REML) to fit a generalized least squares (GLS) linear model with the GLS function of Pinheiro & Bates (2000), which enabled us to model heteroscedastic and correlated errors. This initial model contained the time (day), the variables retained by the PCA (T_s, θ, u_* and

VPD) with their associated quadratic terms, and appropriate interactions to test our hypotheses (i.e. two-way interactions between MICROHABITAT, T_s, θ and u_* and two- to three-way interactions between SEASON, T_s and θ). Regarding heteroscedasticity, prior data exploration revealed that the variance of χ_s increased globally with smaller VPD. Therefore, we used this variable as a variance covariate; that is, by including it in the variance structure of the model to allow a spread of residuals proportional to VPD^{-1} as suggested by the procedure of Zuur *et al.* (2009). To ensure normality, a Box–Cox transformation was applied on χ_s. After that, the model was refitted with a linear mixed effects (LME) model including a random intercept that varied with LOCATION. This was done with the LME function of Pinheiro & Bates (2000), which has the same features as the GLS function, but in addition enables random effects to be modelled. That made it possible to compare the GLS and LME models as nested and thus to test the significance of the added random effect with a likelihood ratio (LR) test. More complex random structures were also explored in the same way (random intercept correlated or not with time as a random slope). Afterwards, a backward variable selection was carried out. This was achieved by refitting the model with maximum likelihood (ML), dropping each term one by one and comparing the nested models. Because MICROHABITAT and SEASON had more than two levels, an LR test was preferred over the *t*-statistic as the selection criterion. During the selection process, insignificant fixed terms involved in significant higher-order terms were retained in the model. The selection was finalized once all terms were significant. The final model R^2 was calculated according to Johnson (2014), and multicollinearity was assessed with the condition number (Belsley, 2006).

For the whole study period and each season, θ, T_s, χ_s and F_s were tested for differences in microhabitat (after applying a Box–Cox transformation on θ, T_s and χ_s, and a Yeo–Johnson transformation on F_s) by using the same modelling strategy.

Finally, F_s was upscaled to the ecosystem scale by considering the fraction that each microhabitat covered for the footprint of the eddy covariance tower (Barron-Gafford *et al.*, 2011). The error in ecosystem-F_s was considered to be 7.5%, corresponding to sampling for F_s with a manual chamber every 2 months for calibration of the empirical soil CO_2 transfer coefficient (Sánchez-Cañete *et al.*, 2017).

Wavelet analysis

To understand patterns of variation in χ_s in time and frequency, we performed a wavelet analysis on data averaged hourly. This technique has already been used and described for F_s research; in particular, the wavelet coherence analysis is preferable to other traditional spectral decompositions such as the Fourier approach when the time series show clear signs of non-stationarity and heteroscedasticity (Vargas *et al.*, 2010). We used a continuous wavelet transform with the Morlet mother wavelet to split up every χ_s sequence and their main controlling factors in a time-period space to obtain their wavelet power spectra (WPS). On the one hand, every WPS was averaged over time for each period to obtain the global wavelet power spectra (GWPS) (for plant species with replicates, the GWPS was calculated from an inter-individual mean of WPS). On the other hand, we determined the wavelet coherence between χ_s signals and each variable, corresponding to their local covariance in the time-period space standardized by the product of their WPS at each measurement location. When necessary, the partial wavelet coherence was preferred to inspect the local correlation after removing the confounding effect of another variable (Ng & Chan, 2012). The phase relation was also calculated for each pair of time series. All significant regions ($\alpha = 0.05$) in the time-period space were estimated by comparison with a null model based on 1000 Monte Carlo randomizations.

Results

Global trends

Soil CO_2 molar fractions (χ_s) were variable in time and space, as shown by their coefficients of variation (Table 1). In space, intra-microhabitat variation was always larger than inter-microhabitat variation (9–15 and 2–5%, respectively). Temporal variation (15–52%) was always equal to or greater than spatial variation, with a maximum during the dry season. Temporal

Table 1 Spatio-temporal variation in soil CO_2 molar fraction

	Inter-season			Growing season			Dry season		
Microhabitat	Mean / μmol mol^{-1}	SV / %	TV / %	Mean / μmol mol^{-1}	SV / %	TV / %	Mean / μmol mol^{-1}	SV / %	TV / %
Bare soil	769	–	20	820	–	21	551	–	52
Festuca sp.	779	9	23	805	13	17	557	9	36
Hormatophylla sp.	704	15	22	775	15	17	569	12	41
Genista sp.	788	–	17	813	–	15	583	–	28
Inter-microhabitat	760	5	21	803	2	18	565	2	40

SV, spatial coefficient of variation; TV, temporal coefficient of variation. The TV for composite samples (*Festuca* sp., *Hormatophylla* sp. and 'inter-microhabitat') was calculated from the pooled standard deviation for equal sample sizes, $\sigma_{pooled} = \sqrt{\frac{\sigma_1+\sigma_2+\ldots+\sigma_k}{k}}$ where σ_k are the standard deviations of the k samples.

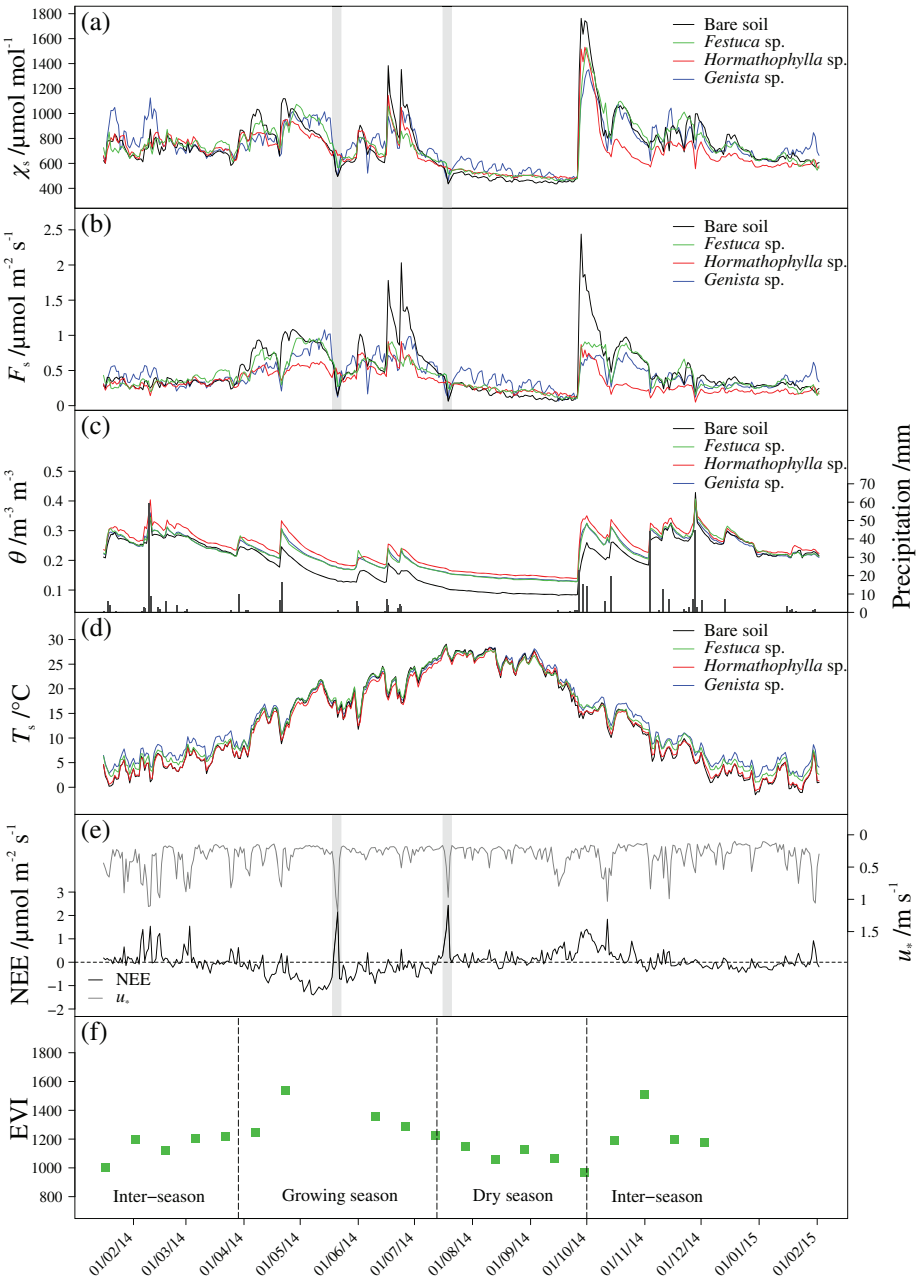

Figure 1 Daily averaged time series of: (a) soil CO_2 molar fractions (χ_s), (b) soil CO_2 effluxes (F_s), (c) soil water content (θ) and precipitation (vertical bars), (d) soil temperature (T_s), (e) net ecosystem exchange (NEE) and friction velocity (u_*) and (f) time series of the enhanced vegetation index (EVI) obtained at 16-day intervals. Shaded areas delimit clear ventilation events (i.e. ecosystem CO_2 emissions >2 µmol m^{-2} s^{-1} during soil drying concomitant with decreases in χ_s and F_s).

variation in χ_s and soil CO_2 effluxes (F_s) mainly followed variation in soil water content (θ) resulting from precipitation (Figure 1a–c). Soil temperature (T_s) followed a clear annual cycle (Figure 1d). Differences in χ_s, F_s, θ and T_s between microhabitats were not significant, regardless of the time interval tested. Sharp increases in net ecosystem exchange often coincided with strong friction velocity (u_*) episodes from wind; in particular, two ventilation events were clearly identifiable in May and July (i.e. CO_2 loss from soil driven by wind) (Figure 1e). Over 1 year, the ecosystem carbon balance was almost neutral (0 ± 5 g C m^{-2}); however, the ecosystem was a net carbon sink during the growing season (uptake of 43 ± 4 g C m^{-2}) and a source during the dry and inter-seasons (emissions of 24 ± 1 and 20 ± 3 g C m^{-2}, respectively). Maximum ecosystem carbon uptake during the growing season coincided with a maximum enhanced vegetation index (EVI), whereas maximum ecosystem carbon emissions at the end of the dry season coincided with minimum EVI (Figure 1f), soil rewetting and sharp increases in χ_s and F_s.

Explanatory model of dynamics of soil CO_2 molar fraction

The Box–Cox-transformed χ_s dynamics was described best by a linear mixed model incorporating a random intercept of sampling location correlated with time as a random slope (LR = 731, degrees

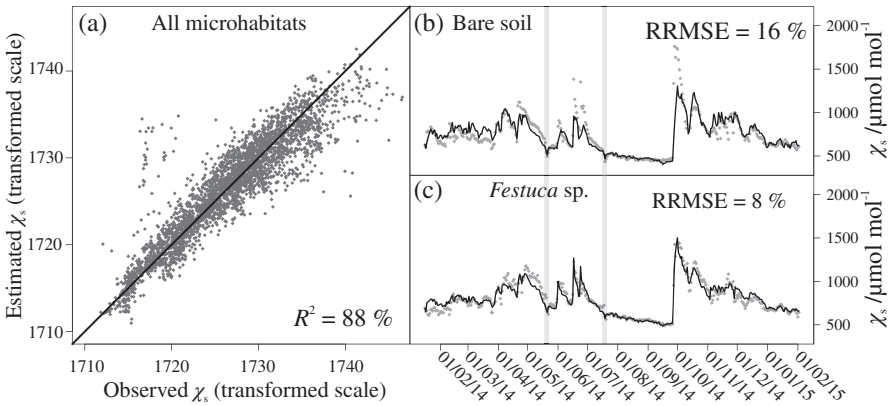

Figure 2 Values of the fitted model of soil CO_2 molar fraction (χ_s). (a) Plotted against observations for all microhabitats (all χ_s are Box–Cox transformed). Black line is the 1:1 line. Results are based on $n = 3064$ daily observations (dark points). (b and c) Over time for bare soil and a plant of *Festuca* sp., respectively (after back-transforming χ_s to the original scale). Shaded areas delimit clearly identified ventilation events. RRMSE, relative root mean square error, defined here as the root mean square error divided by the observation mean. At each microhabitat, results are based on $n = 383$ daily observations (grey points).

of freedom (d.f.) = 3, $P < 0.0001$). This kind of model has the general form:

$$\mathbf{y} = \mathbf{X}\,\boldsymbol{\beta} + \mathbf{Z}\,\mathbf{u} + \varepsilon, \tag{2}$$

where $\mathbf{y}$ is a vector of transformed χ_s, $\mathbf{X}\,\boldsymbol{\beta}$ is the model's fixed part with $\mathbf{X}$ being the design matrix of the fixed explanatory variables and $\boldsymbol{\beta}$ a vector of regression coefficients associated with the fixed effects, $\mathbf{Z}\,\mathbf{u}$ is the model's random part with $\mathbf{Z}$ being the design matrix of the random explanatory variables and $\mathbf{u}$ a vector of regression parameters associated with the random effects, and ε is the residual.

Our model explained 88% of the variance in the data, of which 65% was attributable to the fixed component. The model condition number was < 30 (equal to 9), which ruled out issues of multicollinearity. After back-transforming the fitted model values, the root mean square error and relative root mean square error were 98 µmol mol^{-1} and 13%, respectively. The fitted model is presented on a transformed scale for all microhabitats (Figure 2a) and on the original scale for the dominant microhabitats (Figure 2b,c). The χ_s decreased noticeably during the ventilation events identified and were taken into account by the model.

The fixed part of the model (Table 2) highlighted neither significant variation in mean χ_s with seasons (LR = 0.6, d.f. = 2, $P = 0.75$) nor microhabitats (LR = 1.1, d.f. = 3, $P = 0.78$). However, the results showed that the dynamics of χ_s was affected differently by some variables depending on seasons and microhabitats. During the inter-season, T_s was the strongest (positive) controlling factor of χ_s and its effect (φ) was significantly larger for bare soil than plants ($\varphi = 10.15$, compared with $\varphi = 8.53$, $\varphi = 8.67$, $\varphi = 9.06$, respectively). The positive coefficient for T_s^2 ($\varphi = 2.02$) revealed a locally convex relation between T_s and χ_s. The second most important (positive) controlling factor of χ_s was θ. Bare soil was the microhabitat where χ_s were the most sensitive to the variation in θ ($\varphi = 6.90$). By contrast, θ had a minimal effect for *Hormathophylla* sp. ($\varphi = 3.19$). The negative coefficient of θ^2 ($\varphi = -1.25$) highlighted a locally concave relation between θ and χ_s. The third (negative) controlling factor of χ_s was u_*. In plants, χ_s were always less responsive to variation in u_* than in bare soil ($\varphi = -0.17$, $\varphi = -0.57$ and $\varphi = -0.61$ compared with $\varphi = -0.86$). The smallest (negative) controlling factor of χ_s was VPD ($\varphi = -0.42$). During the inter-season, T_s and θ interacted negatively, but weakly (so $\varphi = -0.78$). During the growing season, the effect of T_s decreased ($\varphi = 3.29$) and θ became the main controlling factor of χ_s ($\varphi = 5.41$). In addition, both variables started to interact strongly and positively ($\varphi = 5.58$). During the dry season, the effect of T_s became negative ($\varphi = -2.41$) and the effect of θ intensified ($\varphi = 6.80$).

Refitting the same model after removing terms involving SEASON ($R^2 = 86\%$, data not shown) showed that on an annual scale θ had a predominant effect on χ_s ($\varphi = 6.28$) compared with T_s ($\varphi = 4.22$), and that their interaction was substantial ($\varphi = 1.99$).

Time-frequency patterns of soil CO_2 molar fractions

The global wavelet power spectra of θ, T_s and χ_s revealed their main periodic components among microhabitats (Figure 3a–c, respectively). The soil water content showed strong periodicity on timescales of weeks and months. By contrast, T_s had a pronounced daily periodicity. Consequently, χ_s periodicity was essentially a combination of the principal periodic components of θ and T_s. Overall, major power peaks occurred around the same periods regardless of microhabitat.

For the time-period correlations between χ_s and their main controlling factors identified, we show only wavelet or partial wavelet coherence spectra of bare soil and one plant of *Festuca* sp. (Figure 4) to simplify the display of results, but we compare all spectra. The correlation between χ_s and their main controlling factors was always significantly larger (reddish areas) at specific periodicities. However, at a given periodicity, those correlations were not continuous over the study (i.e. reddish areas were discontinuous over time). Areas of strong significant correlation between χ_s and θ (Figure 4a,b) corresponded to major rain events (Figure 1c). During these events, the correlation intensity and periodicity varied according to rain pulses and microhabitats. They were larger (with a periodicity up to months) under specific conditions: (i) when precipitation followed a relatively dry and hot interval, especially during rain at the end of the dry season and to a lesser extent during the growing season and (ii) for bare soil than plants. In particular, a strong correlation between χ_s and θ was detectable earlier during rain pulses in bare soil in the growing season. Globally, χ_s and θ

Table 2 Summary of fixed effects of explanatory model of soil CO_2 molar fraction

Model fixed effect	Compared factor level	β	SE	φ
Intercept		**1731.3**	1.65	1731.3
Microhabitat	Bare soil	0.19	3.26	1731.5
	Genista sp.	0.73	3.26	1732.0
	Hormatophylla sp.	−1.37	2.30	1729.9
Season	Growing	−0.09	0.36	1731.2
	Dry	0.34	0.60	1731.6
T_s^2		**2.02**	0.22	2.02
T_s		**8.67**	0.45	8.67
T_s • Season	Growing	**−5.38**	0.56	3.29
	Dry	**−11.08**	1.18	−2.41
T_s • Microhabitat	Bare soil	**1.48**	0.32	10.15
	Genista sp.	0.39	0.30	9.06
	Hormatophylla sp.	−0.14	0.21	8.53
θ^2		**−1.25**	0.06	−1.25
θ		**4.05**	0.30	4.05
θ • Season	Growing	**1.36**	0.35	5.41
	Dry	**2.75**	0.37	6.80
θ • Microhabitat	Bare soil	**2.85**	0.32	6.90
	Genista sp.	−0.15	0.28	3.90
	Hormatophylla sp.	**−0.86**	0.19	3.19
T_s • θ		**−0.78**	0.27	−0.78
T_s • θ • Season	Growing	**6.36**	0.44	5.58
	Dry	0.92	0.65	0.14
u_*		**−0.57**	0.05	−0.57
u_* • Microhabitat	Bare soil	**−0.29**	0.10	−0.86
	Genista sp.	−0.04	0.10	−0.61
	Hormatophylla sp.	**0.40**	0.07	−0.17
VPD		**−0.42**	0.07	−0.42

Bold numbers, *P*-value < 0.01; θ, soil water content; T_s, soil temperature; u_*, friction velocity; VPD, vapour pressure deficit; $\boldsymbol{\beta}$, vector of regression coefficients β; SE, standard error of β; φ, the absolute fixed effect.
Prior to modelling, the response variable was Box–Cox-transformed, and quantitative explanatory variables were standardized (centred and scaled to zero mean and unit variance). The model takes *Festuca* sp. and inter-season as baselines to generate β. Therefore, the intercept is the absolute estimated mean for those factor levels. For strictly quantitative terms, β is also an absolute estimate corresponding to those baselines. By contrast, for terms involving factors, β describes relative variations from the baseline β of the considered factor. In the last column, to facilitate comparison within factors, we computed all the remaining absolute effects (i.e. means and slopes) for every factor level. Results are based on $n = 3064$ observations.

varied in phase, except for a major rainfall event during the second inter-season when signals were negatively correlated. Further data inspection showed that such phase inversions occurred during other rainfall events, but were not revealed by the wavelet analysis, apparently because of their smaller magnitude. However, decreases in χ_s were generally greater during rain events exceeding 30 mm.

The correlation between χ_s and T_s (Figure 4c,d) was significantly larger for hourly to daily periodicities. It was also markedly intermittent for larger periodicities (from days to weeks), generally after rain. The autumn rain pulses only, which marked the transition between the dry season and inter-season, were able to induce a

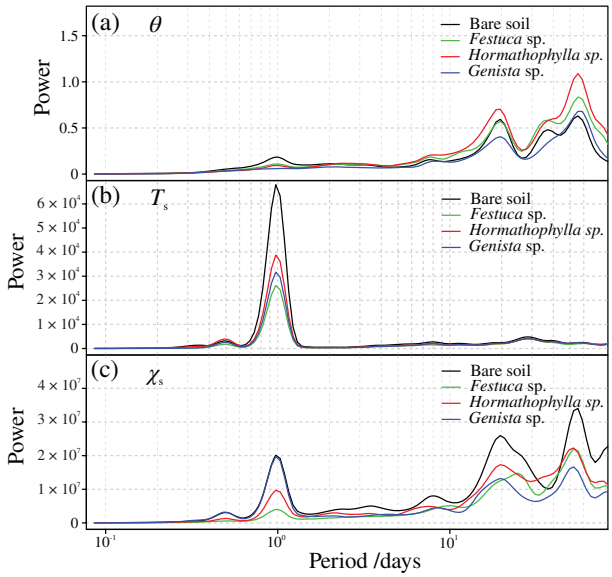

Figure 3 Global wavelet power spectra by microhabitat of (a) soil water content (θ), (b) soil temperature (T_s) and (c) soil CO_2 molar fraction (χ_s). Results are based on $n = 9210$ hourly observations.

strong correlation for a periodicity up to months. Moreover, later during the inter-season when χ_s started to correlate with T_s at large periodicities (weeks to months) in all plants, such correlation was absent in bare soil. In general, χ_s and T_s varied in phase, but were occasionally negatively correlated during the dry season. For periodicities greater than 1 day, variation in T_s usually led to variation in χ_s, suggesting a control of T_s on χ_s.

Areas of significantly stronger correlation between χ_s and u_* (Figure 4e,f) essentially occurred at periodicities of a few days during large u_* values (Figure 1e), but this correlation was weaker in *Hormathophylla* sp. (data not shown). Usually, χ_s and u_* were negatively correlated and variation in u_* often tended to lead to variation in χ_s for periodicities ranging from hours to months, suggesting a controlling effect of u_* on χ_s.

Upscaling soil CO_2 efflux from the microhabitat to ecosystem

By upscaling F_s from the microhabitat to the ecosystem, it was estimated that 175 ± 13 g C m^{-2} were emitted at the experimental site in 1 year. By comparison, 155 ± 8 g C m^{-2} were estimated to have been emitted through ecosystem respiration (R_{eco}). Both fluxes followed the same trend, but diverged strongly during progressive soil drying from the mid-growing season through to the dry season (Figure 5). In particular, during the driest period in August ($\theta = 0.11$ (0.03) m^{-3} m^{-3}, given as mean (spatial standard deviation)), R_{eco} was ca. 0 g C m^{-2}, whereas F_s varied spatially from 0.1 g C m^{-2} to 0.4 g C m^{-2} (in plants of *Hormatophylla* sp. and *Festuca* sp., respectively).

Discussion

This study identified soil water content (θ), soil temperature (T_s) and friction velocity (u_*) as the main biophysical controlling

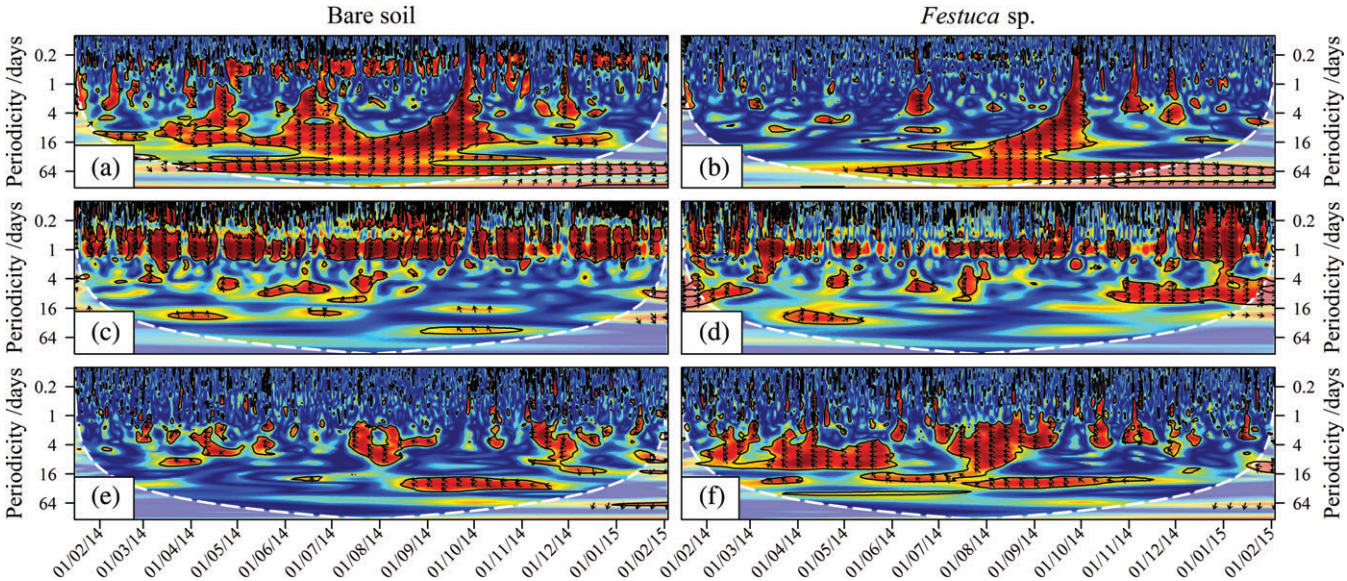

Figure 4 Spectra from wavelet coherence analysis between soil CO_2 molar fraction (χ_s) and its main controlling factors for bare soil and a plant of *Festuca* sp. (a and b) Soil water content (θ). (c and d) Soil temperature (T_s). (e and f) Friction velocity (u_*). In (c) and (d) simple wavelet coherence was used, whereas in (a), (b), (e) and (f) partial wavelet coherence was used to remove the potential confounding daily effect of T_s on χ_s. The correlation intensity varies from blue (low) to red (high) and areas of significant correlations are delimited by a thin black line. Phase relations are represented for large correlations only (i.e. squared wavelet coherence coefficient > 0.7). Arrows pointing left or right mean antiphase or phase, respectively. Arrows pointing upwards or downwards mean that variation of the considered variable leads or lags χ_s variation, respectively. The white dashed line delimits the cone of influence, defined as the area in which the reliability of results does not suffer from edge effects (i.e. errors at the beginning and at the end of the spectra due to the inherent finite length of the time series while the analysis assumes data to be cyclic). Results are based on $n = 9210$ hourly observations.

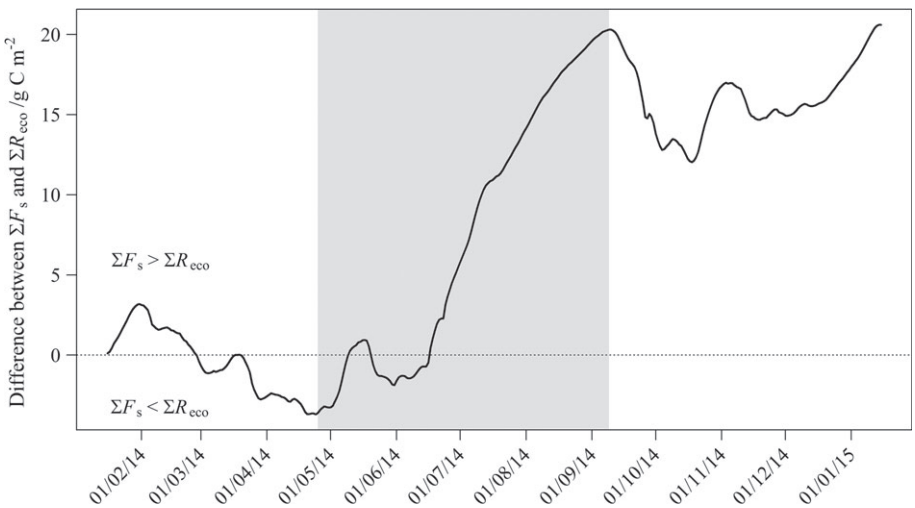

Figure 5 Difference between cumulative ecosystem-scale soil CO_2 efflux ($\sum F_s$) and cumulative ecosystem respiration ($\sum R_{eco}$) over a year. The shaded area highlights the period of largest divergence between these fluxes.

factors of soil CO_2 molar fractions (χ_s) dynamics, and their effects varied with seasons and microhabitats (Table 2). Even if no significant variation in average χ_s (or of other soil variables) was detected between microhabitats, this lack of significance certainly came from (i) the intra-species variation that was greater than the inter-species variation (potentially as a result of large inherent individual variation or soil heterogeneity) and (ii) the large temporal variability, reducing the sensitivity of statistical tests (Table 1).

The soil water content effect

On an annual scale, the dynamics of χ_s was mainly and positively affected by θ, already reported in water-limited ecosystems regarding soil CO_2 efflux (F_s) (e.g. Almagro *et al.*, 2009). Water regulates root and microbial activity as well as gas and substrate diffusion (Luo & Zhou, 2006). Therefore, large θ favours respiration directly by stimulating biological processes and indirectly by facilitating the transport of soluble metabolic substrates to roots and microorganisms. It also reduces soil air-filled porosity, thus

slowing down CO_2 diffusion and enhancing CO_2 concentrations. The strong correlation between θ and χ_s during rain (Figure 4) revealed the typical pulse response of χ_s to soil wetting in drylands, termed a 'hot moment' (Leon *et al.*, 2014). The concave form of the effect of θ on χ_s reflects a mitigation locally of the effect of θ that could result from limited respiration because of a decrease in availability of metabolic substrate (Sponseller, 2007).

The common periodicity between χ_s and θ of weeks to months (Figure 3) reflects the strong influence of seasonal rainfall on soil CO_2 production (Vargas *et al.*, 2010). From mid-growing season to the end of the dry season, drought reduces plant activity markedly, as reflected by a decrease in enhanced vegetation index (EVI) (Figure 1f). Consequently, the greater sensitivity of χ_s to θ during those moments (Table 2, Figure 4) is mostly attributable to heterotrophic respiration (R_h), which is certainly magnified by the Birch effect, a burst in CO_2 in response to rewetting of previously dry soil that has been attributed to a rapid mineralization of either dead microbial biomass or osmoregulatory substances released by soil microorganisms in response to osmotic stress (Unger *et al.*, 2010). In addition, drying and rewetting cycles can destabilize soil aggregates and thus increase metabolic substrate availability for microorganisms (Austin *et al.*, 2004). Therefore, future trends of drying and precipitation patterns that were more concentrated in heavy rainfall events predicted for the area (Argüeso *et al.*, 2012) could considerably enhance the pulse response of χ_s to θ.

The negative correlation between χ_s and θ during strong inter-season rainfall (Figure 4) was due to a rapid decrease in χ_s. This might arise from two processes: (i) rapid water infiltration can physically expel CO_2-rich air from soil and (ii) the dissolution of soil CO_2 in rainwater can be favoured momentarily by disequilibrium between CO_2-poor rainwater and relatively large soil CO_2 concentration. The first process contributes to the release of CO_2 towards the atmosphere, whereas the second can sequester it if dissolved CO_2 reaches aquifers. Other substantial decreases in χ_s during rain events exceeding 30 mm suggest that a substantial amount of precipitation is necessary for the process to occur.

The greater sensitivity of χ_s to θ in bare soil revealed a greater effect of rewetting in this microhabitat, also described by Almagro *et al.* (2009) regarding F_s. We suggest that this could be due to (i) the exposure of bare soil to solar radiation (faster drying and more intense photodegradation can enhance the Birch effect; this might be why the effect of θ on χ_s was detectable only in bare soil at the beginning of the growing season) (Figure 4) and (ii) a greater sensitivity of heterotrophic (R_h) than autotrophic (R_a) respiration to θ. In water-limited ecosystems, R_h is known to respond quickly to even small pulses of rain because of the distribution of microorganisms in the topsoil, whereas the response of R_a is delayed and requires greater or repeated rainfall for the water to reach deeper roots (Sponseller, 2007). Metabolic differences between roots and microbes, however, could also be involved, rather than purely a water-limitation effect.

The greater sensitivity of χ_s to θ in *Festuca* sp. than *Hormathophylla* sp. is possibly because of their phenological differences. The senescent feature of *Festuca* sp. during the dry season may increase soil organic matter (SOM), which favours microbial decomposition during soil rewetting. This is supported by the divergence in χ_s and F_s between these species after the first autumn rain pulses (Figure 1a,b). However, physiological differences between the species could also be involved.

The soil temperature effect

On an annual basis, T_s had a secondary and positive effect on χ_s because of its catalytic role in enzyme reactions and thus in respiration (Luo & Zhou, 2006). However, this effect interacted strongly and positively with θ. On the one hand, this means that variation in T_s had a major effect on χ_s when θ increased. Such a pattern was confirmed by the strong correlations between T_s and χ_s starting with rain; in particular, the correlation between large periodicities (weeks to months) during the growing season and autumn rain pulses highlights the importance of T_s during these seasonal events (Figure 4). These time intervals without water limitation stimulate biological reactions which are then catalysed by T_s. Our model revealed this strong interaction only during the growing season and not during the dry season because of our choice of season demarcation. This is because the controlling effect of T_s started with autumn rain pulses, which were chosen to mark the beginning of the inter-season. On the other hand, the interaction between T_s and θ means that variation in θ had a stronger effect when T_s was larger, certainly for the Birch effect, which tends to occur when soil is warm. Overall, the interaction accords with other studies suggesting that F_s models based exclusively on temperature (mostly Q_{10}-like and Arrhenius-like) are not suitable in water-limited ecosystems (e.g. Reichstein *et al.*, 2003; Leon *et al.*, 2014). Additional proof for this statement comes from the negative relations between T_s and χ_s during the dry season, and even when T_s was the main limiting factor of χ_s (inter-season) the effect of θ was still considerable.

Consequently, even if the annual positive effect of T_s on χ_s suggests a positive feedback between climate change and F_s in this ecosystem, future precipitation patterns will probably play a critical role. The predicted drying of the Mediterranean region could mitigate the positive effect of T_s on χ_s, but the potentially larger pulse response of soil respiration to more concentrated heavy rain events complicates predictions.

On a daily scale, the strong periodicity of T_s and its marked positive correlation with χ_s (Figures 3 and 4) suggest that T_s would have a more pronounced effect in a model with higher temporal resolution, although potentially confounded with photosynthesis (Vargas *et al.*, 2010).

The sensitivity of χ_s to T_s was greater in bare soil; this is in contrast with Cable *et al.* (2013), who found greater sensitivity of F_s under plants. We suggest, however, that the distinct pattern reported by the above authors was potentially a special feature of phreatophyte mesquites with great hydraulic lifting capacity (Scott *et al.*, 2008). In our ecosystem, the observed pattern could be due to a greater sensitivity of R_h to T_s than R_a. This might

arise from the following. (i) Greater tolerance of drought by microorganisms; thus they responded more easily to T_s. (ii) The seasonality of plant activity. The strong correlation with high periodicity between χ_s and T_s following the first autumn rain events, which was observed among plants but not in bare soil, suggests that plants were recovering from the adverse effect of the dry season. This is supported by the increase in EVI and neutralization of net ecosystem exchange at this time, indicating a recovery of photosynthesis and carbon fixation (Figure 1e,f). (iii) An indirect effect of photodegradation, which might supply more labile substrates to microorganisms in bare soil. Consequently, when moisture conditions become favourable, the response of R_h to T_s might be enhanced by the availability of resources. (iv) Poorer SOM quality in bare soil because plants provide litter and root exudates to the soil. However, poor SOM quality can speed up microbial decomposition (Bosatta & Ågren, 1999). The similar sensitivity of χ_s to T_s among microhabitats with different plant cover also suggests that the response of R_a to T_s might not vary with species composition in this ecosystem, possibly as a result of drought adaptation.

The wind effect

The model developed corroborated the transport of soil CO_2 by ventilation in this ecosystem (Sánchez-Cañete *et al.*, 2011). The dominant correlation between χ_s and u_* for periodicities of a few days indicates that synoptic cycles of atmospheric pressure might be the underlying governing factor (Figure 4e,f).

The greater sensitivity of χ_s to u_* in bare soil than in plants possibly results from more exposure of this microhabitat to atmospheric turbulence. In contrast, the plant cover forms a natural boundary that might limit wind penetration into soil pores. These results emphasize that ventilation is a spatially heterogeneous process.

Upscaling F_s from the microhabitat to ecosystem

Our annual upscaled ecosystem-F_s (175 ± 13 g C m^{-2}) was closer to values with small ranges estimated in desert shrubs (Luo & Zhou, 2006) (224 ± 38 g C m^{-2}). Because our site is less arid, soil respiration could also be restricted here by cold, altitude or edaphic conditions. In particular, the cementing activity of calcium carbonate and iron oxides might protect a fraction of SOM from decomposition (Oyonarte *et al.*, 1994).

Our annual estimate of ecosystem-F_s exceeding ecosystem respiration (R_{eco}) supports similar results pointing out issue(s) in the measurement or calculation of those fluxes, the causes of which are still a matter of debate (Barba *et al.*, 2017). We acknowledge that our ecosystem-F_s was potentially overestimated because of few spatial replicates; in particular, more replicates are necessary for bare soil and *Genista* sp. to validate results involving those microhabitats. However, there have been few annual estimates of F_s based on continuous measurements so far, and because temporal variation was 4–20 times greater than spatial inter-microhabitat variation (coefficients of variation of 21 and 40%, and 5 and 2% respectively; Table 1), we believe we have obtained a reliable estimate. The strong divergence between ecosystem-F_s and R_{eco} during soil drying (Figure 5) and the unlikely almost zero values of R_{eco} suggest that (i) the calculation of R_{eco} might give too much importance to respiration controlled by temperature, neglecting the effect of θ on CO_2 diffusion (although respiration diminishes with drought, diffusion is enhanced by more air-filled porosity), and (ii) carbonate precipitation favoured by the decrease in θ could have maintained a substantial basal F_s during the dry season, and the use of temperature alone to model R_{eco} might be inadequate to represent such an abiotic process. A better estimate of R_{eco} and or ecosystem-F_s would enable aboveground R_a to be deduced from the difference between those fluxes. Chamber measurements and stable carbon isotope techniques could help to discriminate between R_a, R_h and abiotic CO_2 production to improve the accuracy of flux partitioning.

Conclusion

Soil water content (θ) was overall the main factor controlling the dynamics of soil CO_2 molar fractions (χ_s). Soil temperature (T_s) became the first limiting factor of χ_s only during the inter-season, but the effect of θ was still substantial. In addition, the strong interaction between T_s and θ confirmed that models based on temperature alone are inappropriate in water-limited ecosystems. In particular, dry and hot intervals greatly enhanced the pulsed response of χ_s to precipitation (Birch effect). The friction velocity was also identified in this study as a significant predictor of χ_s dynamics. The microhabitat modulated the response of χ_s to its main controlling factors identified. Our upscaling of F_s from the microhabitat to the ecosystem highlights a discrepancy between R_{eco} and ecosystem-F_s. Continuous automated measurements greatly improved our understanding of the temporal patterns governing χ_s and should now be used with greater spatial coverage in conjunction with chamber measurements and stable carbon isotope techniques to improve ecosystem CO_2 flux modelling and partitioning.

Supporting Information

The following supporting information is available in the online version of this article:

Text S1. Principal component analysis.

Table S1. Eigenvalues and percentage variance accounted for by each principal component

Figure S1. Variable selection during principal component analysis on (a) the first principal component, (b) the second principal component and (c) the third principal component.

Figure S2. Correlations between the variables and PCs 1 and 2 plotted in a unit circle and (b) PC scores plotted in the plane of principal components 1 and 2.

Acknowledgements

These data were funded by the Spanish Ministry of Economy and Competitiveness projects SOILPROF (CGL2011-15276-E) and GEISpain (CGL2014-52838-C2-1-R) and the European

Commission project DIESEL (PEOPLE-2013-IOF-625988). We acknowledge the DINCOS project (Biocrust Dynamics, key CGL2016-78075-P) funded by the Spanish State Plan for Scientific and Technical Research and Innovation 2013–2016, which funds the first author. C. J. R. Lopez thanks the PhD program in Earth Sciences (University of Granada) in which he is enrolled and Gilles Le Moguedec for his advice on statistics. We thank the editor and three anonymous reviewers for useful comments and suggestions, which improved the manuscript.

References

Almagro, M., López, J., Querejeta, J. & Martínez-Mena, M. 2009. Temperature dependence of soil CO_2 efflux is strongly modulated by seasonal patterns of moisture availability in a Mediterranean ecosystem. *Soil Biology & Biochemistry*, **41**, 594–605.

Argueso, D., Hidalgo-Munoz, J., Gamiz-Fortis, S., Esteban-Parra, M. & Castro-Diez, Y. 2012. High-resolution projections of mean and extreme precipitation over Spain using the WRF model (2070–2099 versus 1970–1999). *Journal of Geophysical Research: Atmospheres*, **117**, D12108, https://doi.org/10.1029/2011JD017399.

Austin, A.T., Yahdjian, L., Stark, J.M., Belnap, J., Porporato, A., Norton, U. *et al.* 2004. Water pulses and biogeochemical cycles in arid and semiarid ecosystems. *Oecologia*, **141**, 221–235.

Bahn, M., Reichstein, M., Davidson, E.A., Grünzweig, J., Jung, M., Carbone, M. *et al.* 2010. Soil respiration at mean annual temperature predicts annual total across vegetation types and biomes. *Biogeosciences*, **7**, 2147–2157.

Barba, J., Cueva, A., Bahn, M., Barron-Gafford, G.A., Bond-Lamberty, B., Hanson, P.J. *et al.* 2017. Comparing ecosystem and soil respiration: review and key challenges of tower-based and soil measurements. *Agricultural and Forest Meteorology*, **249**, 434–443.

Barron-Gafford, G.A., Scott, R.L., Jenerette, G.D. & Huxman, T.E. 2011. The relative controls of temperature, soil moisture, and plant functional group on soil CO_2 efflux at diel, seasonal, and annual scales. *Journal of Geophysical Research: Biogeosciences*, **116**, G01023, https://doi.org/10.1029/2010JG001442.

Belsley, D.A. 2006. *Conditioning Diagnostics*. John Wiley & Sons, New York, NY.

Bond-Lamberty, B. & Thomson, A. 2010. A global database of soil respiration data. *Biogeosciences*, **7**, 1915–1926.

Bosatta, E. & Ågren, G.I. 1999. Soil organic matter quality interpreted thermodynamically. *Soil Biology & Biochemistry*, **31**, 1889–1891.

Cable, J.M., Ogle, K., Barron-Gafford, G.A., Bentley, L.P., Cable, W.L., Scott, R.L. *et al.* 2013. Antecedent conditions influence soil respiration differences in shrub and grass patches. *Ecosystems*, **16**, 1230–1247.

Etiope, G. 1999. Subsoil CO_2 and CH_4 and their advective transfer from faulted grassland to the atmosphere. *Journal of Geophysical Research: Atmospheres*, **104**, 16889–16894.

Hamerlynck, E.P., Scott, R.L., Sánchez-Cañete, E.P. & Barron-Gafford, G.A. 2013. Nocturnal soil CO_2 uptake and its relationship to subsurface soil and ecosystem carbon fluxes in a Chihuahuan Desert shrubland. *Journal of Geophysical Research: Biogeosciences*, **118**, 1593–1603.

Hashimoto, S., Carvalhais, N., Ito, A., Migliavacca, M., Nishina, K. & Reichstein, M. 2015. Global spatiotemporal distribution of soil respiration modeled using a global database. *Biogeosciences*, **12**, 4121–4132.

Johnson, P.C. 2014. Extension of Nakagawa & Schielzeth's R^2_{GLMM} to random slopes models. *Methods in Ecology and Evolution*, **5**, 944–946.

Kowalski, A.S. & Argüeso, D. 2011. Scalar arguments of the mathematical functions defining molecular and turbulent transport of heat and mass in compressible fluids. *Tellus B*, **63**, 1059–1066.

Kowalski, A.S., Serrano-Ortiz, P., Janssens, I.A., Sánchez-Moral, S., Cuezva, S., Domingo, F. *et al.* 2008. Can flux tower research neglect geochemical CO_2 exchange? *Agricultural and Forest Meteorology*, **148**, 1045–1054.

Leon, E., Vargas, R., Bullock, S., Lopez, E., Panosso, A.R. & La Scala, N. 2014. Hot spots, hot moments, and spatio-temporal controls on soil CO_2 efflux in a water-limited ecosystem. *Soil Biology & Biochemistry*, **77**, 12–21.

Lloyd, J. & Taylor, J. 1994. On the temperature dependence of soil respiration. *Functional Ecology*, **8**, 315–323.

Luo, Y. & Zhou, X. 2006. *Soil Respiration and the Environment*. Academic Press, Burlington, MA.

Ma, J., Liu, R., Tang, L.-S., Lan, Z.-D. & Li, Y. 2014. A downward CO_2 flux seems to have nowhere to go. *Biogeosciences Discussions*, **11**, 10419–10450.

Ng, E.K. & Chan, J.C. 2012. Geophysical applications of partial wavelet coherence and multiple wavelet coherence. *Journal of Atmospheric and Oceanic Technology*, **29**, 1845–1853.

Niinistö, S., Kellomäki, S. & Silvola, J. 2011. Seasonality in a boreal forest ecosystem affects the use of soil temperature and moisture as predictors of soil CO_2 efflux. *Biogeosciences*, **8**, 3169–3186.

Oyonarte, C., Pérez-Pujalte, A., Delgado, G., Delgado, R. & Almendros, G. 1994. Factors affecting soil organic matter turnover in a Mediterranean ecosystems from Sierra de Gádor (Spain): an analytical approach. *Communications in Soil Science and Plant Analysis*, **25**, 1929–1945.

Pinheiro, J.C. & Bates, D.M. 2000. *Mixed-Effects Models in S and S-Plus*. Springer-Verlag New York, New York, NY.

Pumpanen, J., Ilvesniemi, H. & Hari, P. 2003. A process-based model for predicting soil carbon dioxide efflux and concentration. *Soil Science Society of America Journal*, **67**, 402–413.

Raich, J. & Schlesinger, W.H. 1992. The global carbon dioxide flux in soil respiration and its relationship to vegetation and climate. *Tellus B*, **44**, 81–99.

R Core Team 2017. *R: A Language and Environment for Statistical Computing*. R Foundation for Statistical Computing, Vienna [WWW document]. URL https://www.r-project.org/.

Reichstein, M., Rey, A., Freibauer, A., Tenhunen, J., Valentini, R., Banza, J. *et al.* 2003. Modeling temporal and large-scale spatial variability of soil respiration from soil water availability, temperature and vegetation productivity indices. *Global Biogeochemical Cycles*, **17**, 1104, https://doi.org/10.1029/2003GB002035, 4.

Rutledge, S., Campbell, D.I., Baldocchi, D. & Schipper, L.A. 2010. Photodegradation leads to increased carbon dioxide losses from terrestrial organic matter. *Global Change Biology*, **16**, 3065–3074.

Sánchez-Cañete, E.P., Serrano-Ortiz, P., Kowalski, A.S., Oyonarte, C. & Domingo, F. 2011. Subterranean CO_2 ventilation and its role in the net ecosystem carbon balance of a karstic shrubland. *Geophysical Research Letters*, **38**, L09802, https://doi.org/10.1029/2011GL047077.

Sánchez-Cañete, E.P., Kowalski, A.S., Serrano-Ortiz, P., Pérez-Priego, O. & Domingo, F. 2013. Deep CO_2 soil inhalation/exhalation induced by synoptic pressure changes and atmospheric tides in a carbonated semiarid steppe. *Biogeosciences Discussions*, **10**, 5591–5618.

Sánchez-Cañete, E.P., Oyonarte, C., Serrano-Ortiz, P., Curiel Yuste, J., Pérez-Priego, O., Domingo, F. *et al.* 2016. Winds induce CO_2 exchange with the atmosphere and vadose zone transport in a karstic ecosystem. *Journal of Geophysical Research: Biogeosciences*, **121**, 2049–2063.

Sánchez-Cañete, E.P., Scott, R.L., Haren, J. & Barron-Gafford, G.A. 2017. Improving the accuracy of the gradient method for determining soil carbon dioxide efflux. *Journal of Geophysical Research: Biogeosciences*, **122**, 50–64.

Scott, R.L., Cable, W.L. & Hultine, K.R. 2008. The ecohydrologic significance of hydraulic redistribution in a semiarid savanna. *Water Resources Research*, **44**, W02440, https://doi.org/10.1029/2007WR006149.

Serrano-Ortiz, P., Domingo, F., Cazorla, A., Were, A., Cuezva, S., Villagarcía, L. *et al.* 2009. Interannual CO_2 exchange of a sparse Mediterranean shrubland on a carbonaceous substrate. *Journal of Geophysical Research: Biogeosciences (2005–2012)*, **114**, G04015, https://doi.org/10.1029/2009JG000983.

Šimůnek, J. & Suarez, D.L. 1993. Modeling of carbon dioxide transport and production in soil: 1. Model development. *Water Resources Research*, **29**, 487–497.

Soil Survey Staff 1999. *Soil Taxonomy: A Basic System of Soil Classification for Making and Interpreting Soil Surveys*. Natural Resources Conservation Service, Washington, DC.

Sponseller, R.A. 2007. Precipitation pulses and soil CO_2 flux in a Sonoran Desert ecosystem. *Global Change Biology*, **13**, 426–436.

Stekhoven, D.J. & Bühlmann, P. 2012. MissForest – non-parametric missing value imputation for mixed-type data. *Bioinformatics*, **28**, 112–118.

Unger, S., Máguas, C., Pereira, J.S., David, T.S. & Werner, C. 2010. The influence of precipitation pulses on soil respiration–assessing the "Birch effect" by stable carbon isotopes. *Soil Biology & Biochemistry*, **42**, 1800–1810.

Vargas, R., Detto, M., Baldocchi, D.D. & Allen, M.F. 2010. Multiscale analysis of temporal variability of soil CO_2 production as influenced by weather and vegetation. *Global Change Biology*, **16**, 1589–1605.

Vargas, R., Carbone, M.S., Reichstein, M. & Baldocchi, D.D. 2011. Frontiers and challenges in soil respiration research: from measurements to model-data integration. *Biogeochemistry*, **102**, 1–13.

Weisbrod, N., Dragila, M.I., Nachshon, U. & Pillersdorf, M. 2009. Falling through the cracks: the role of fractures in Earth-atmosphere gas exchange. *Geophysical Research Letters*, **36**, L02401, https://doi.org/10.1029/2008GL036096.

Zuur, A., Ieno, E.N., Walker, N., Saveliev, A.A. & Smith, G.M. 2009. *Mixed Effects Models and Extensions in Ecology with R*. Springer Science & Business Media, New York, NY.